Journal of Statistical Physics, Vol. 70, Nos. 5/6, 1993

Surface-Driven Instability and Enhanced Relaxation in the Dynamics of a Nonequilibrium Interface

Chuck Yeung,[1] J. L. Mozos,[2] A. Hernánez-Machado,[1,2] and David Jasnow[1]

Received July 13, 1992; final September 22, 1992

We determine the stability of a nonequilibrium interface between two coexisting solid phases in the presence of a weak external field. Starting at the coarse-grained (Cahn–Hilliard) level, we use the method of matched asymptotics to derive the macroscopic interfacial dynamics. We then show that the external field leads to an instability due to flux along the interface, in contrast with the more common Mullins–Sekerka type instability, which involves fluxes normal to the interface. We also find that the external field produces an important modification of the Gibbs–Thomson relation. With these results, we perform the linear stability analysis for an approximately flat interface. If the field is tangent to the interface, the modification of the Gibbs–Thomson relation is important and the interface is stabilized. If the field is normal to the interface, the surface flux is important, and the effect can be stabilizing or destabilizing, but the orientational dependence is opposite what would be obtained if the Mullins–Sekerka instability dominates. Numerical simulations are performed to study the effect of the surface current and are in agreement with our analytical results.

KEY WORDS: Interfacial dynamics; stability analysis; nonequilibrium steady states.

1. INTRODUCTION

The dynamics of nonequilibrium interfaces is a determining factor in many pattern-forming processes. Familiar examples include directional solidification of binary alloys[1–3] and viscous fingering in Hele–Shaw cells.[4] Important progress has been made in the characterization of the steady-state

[1] Department of Physics and Astronomy, University of Pittsburgh, Pittsburgh, Pennsylvania 15260.

[2] Departament. E.C.M., Facultat de Física, Universitat de Barcelona, E-08028, Barcelona, Spain.

0022-4715/93/0300-1149$07.00/0

patterns and in understanding how these patterns are seleced.[1–4] Likewise, the dynamics of the evolution from the initial state also contain interesting and important features. For example, the stability and shape of the steady-state finger in flow in a rectangular Hele–Shaw cell does not depend on the difference in the viscosities of the two fluids (in the small-surface-tension limit). If, however, the viscosities are equal, the system generally does not evolve toward the single-finger steady state.[5–7] In these problems progress has followed from a description of the interfacial dynamics.[8–12] In particular, if one has a microscopic or coarse-grained description, a first step is often the derivation and analysis of the associated interface equations.[13–17]

In this paper we study the dynamics of an interface between two coexisting solid phases. The system is assumed to be far from criticality and driven out of equilibrium by a weak external field which, through the chosen boundary conditions, induces a flux. We start at the coarse-grained level using the Cahn–Hilliard equation with an additional flux induced by the external field. This model has been used to study both bulk properties[18–21] and the interfacial dynamics[22–26] of driven diffusive systems (DDS)[27–29] and phase ordering dynamics in the presence of a field.[30–32] Using the method of matched asymptotic expansions,[15–17] we derive a *macroscopic* description of the interfacial dynamics from the bulk Cahn–Hilliard equation. For such a description, we need a Gibbs–Thomson relation which relates the deviation of the order parameter near an interface from its coexistence or steady-state value to the local orientation and curvature of the interface. In the absence of a field, the shift in the order parameter is the same on both sides of the interface. We find that the external field produces a novel asymmetry in this shift on the two sides.

For the macroscopic description we also need an expression for the normal velocity of the interface. We show that due to the external field, there is an additional mechanism operative which does not usually arise in the expression for the normal velocity and which can lead to instability. In the more common case of a Mullins–Sekerka instability[9] a small bump on an otherwise flat interface will create a larger gradient in the relevant quantity (e.g., temperature, pressure, or concentration) in front of itself. If the restoring force (such as supplied by surface tension) is not sufficiently large, the bump will grow and the interface is unstable. In our case, the mechanism is not due to such gradients, but rather is due to an imbalance of flux along the interface. The modifications of the Gibbs–Thomson relation and the equation for the normal velocity produce important qualitative changes in the interfacial dynamics. Neither of these effects has been included in previous analyses.[22–24]

Armed with the macroscopic description, we perform a linear stability analysis for a planar interface. We determine the dispersion relation and

find that, at small wavenumbers k, a perturbation h_k of the interfacial position behaves as $|\dot{h}_k/h_k| \sim k^2$ if the field is normal to the interface and $\dot{h}_k/h_k \sim -k^{3/2}$ if the field is tangent to the interface.

More specifically, we find that the surface flux is important if the field in normal to the interface, and it has a stabilizing or destabilizing effect depending on the direction of the field. As will be discussed, the directional dependence is *opposite* that which would be expected from the Mullins–Sekerka instability.[24] The directional dependence when the field is normal to the average interface has been observed in simulations of phase ordering dynamics[31,32] and fingering in driven diffusive systems.[33]

If the external field is parallel to the interface, the modification of the Gibbs–Thomson relation is the most important effect. The external field provides a new relaxation mechanism and stabilizes the interface. Monte Carlo simulations of Leung *et al.*[34] suggest that, for the lattice model, the roughening transition may be raised to (the nonequilibrium) T_c by an external parallel field. Although we use a continuum description, the additional interfacial stabilization in our model could be related to the raising of the roughening temperature in the associated lattice system.

The organization of the remainder of this paper is as follows. In Section 2 we discuss the basic dynamical equations and the planar steady-state solutions. In Section 3 we present the equations describing the macroscopic interfacial dynamics. In the Appendix we derive these equations using the method of matched asymptotic expansions. With the macroscopic description, in Section 4 we consider the linear stability of a planar interface. In Section 5 we study the effect of the enhanced surface flux on the stability of the interface via simulation of the coarse-grained bulk equations. The orientational dependence of the instability is in agreement with our predictions. Section 6 is reserved for concluding remarks.

2. THE MODEL AND STEADY-STATE SOLUTIONS

In this section we discuss a model for a two-phase system in an external field. Let $c(\mathbf{r}, t)$ be the local order parameter at point $\mathbf{r}$ and time t. The order parameter c is positive in one phase, negative in the other, and the interface is at $c = 0$. We take for the equation determining $c(\mathbf{r}, t)$,

$$\frac{\partial c}{\partial t} = \nabla^2 \mu - \mathbf{E} \cdot \nabla \sigma(c) \tag{2.1}$$

where $\mathbf{E}$ is the external field and $\sigma(c)$ is the order-parameter-dependent mobility.[3] The local chemical potential μ is assumed to be of the form

[3] We choose time to have dimensions of (length)^2 and chemical potential μ to have dimensions of concentration c, so the susceptibility $\chi = (\partial \mu/\partial c)^{-1}$ is dimensionless.

$\mu_B - \xi_0^2 \nabla^2 c$, where μ_B does not contain any gradients and ξ_0 is a measure of the interfacial width. For the "standard model," $\mu_B = -c + c^3$. For $\mathbf{E} = 0$ we recover the Cahn–Hilliard equation[35] used in the study of phase ordering dynamics with conserved order parameter.[36]

To interpret the $\mathbf{E}$ dependence we arrive at Eq. (2.1) in two steps. The conserved order parameter $c(\mathbf{r}, t)$ obeys the continuity equation

$$\frac{\partial c(\mathbf{r}, t)}{\partial t} + \nabla \cdot \mathbf{j}(\mathbf{r}, t) = 0 \tag{2.2}$$

where $\mathbf{j}$ is the order parameter current, which we take to be given by

$$\mathbf{j} = -\nabla \mu + \sigma(c)\, \mathbf{E} \tag{2.3}$$

The simplest form of the order-parameter-dependent mobility consistent with Ising-like symmetry is $\sigma(c) = 1 - ac^2$, where a is a constant. More generally, the mobility is large at the interface where c^2 is small and suppressed in the bulk phases. The order parameter dependence leads to the additional term in Eq. (2.1) and is important because the leading E dependence in the current drops out of the continuity equation, Eq. (2.2).[30] In principle, the kinetic coefficient multiplying $\nabla \mu$ should have the same order parameter dependence. For the nonequilibrium steady state, this is unimportant relative to the coupling to the external field and is ignored here. (However, this term would be important if we were considering the equilibrium profile for a system with closed boundary conditions, i.e., walls, rather than open boundary conditions.)

If we assume the "standard model," $\mu = -c + c^3 - \xi_0^2 \nabla^2 c$ and $\sigma(c) = 1 - c^2$, we can obtain, for sufficiently small E, stationary solutions of Eq. (2.1) corresponding to planar interfaces with constant normal flux.[19,24] Let $\hat{\mathbf{n}}$ be the normal to the interface pointing into the "plus" phase and let u be the signed distance to the interface ($u > 0$ in the "plus" domain). The order parameter profile of the stationary solution is

$$c_e(u) = c_\infty(e) \tanh\left(\frac{u}{\xi_e \sqrt{2}}\right) \tag{2.4}$$

where the bulk saturation value $c_\infty(e)$ and interfacial width ξ_e depend on $e \equiv \mathbf{E} \cdot \hat{\mathbf{n}}$ as

$$\begin{aligned} c_\infty^2(e) &= 1 + \sqrt{2}\, \mathbf{E} \cdot \hat{\mathbf{n}} = 1 + \sqrt{2}\, e \\ \xi_e &= \frac{\xi_0}{c_\infty} \end{aligned} \tag{2.5}$$

This analysis can be repeated for more general forms of the chemical potential $\mu = \mu_B - \xi_0^2 \nabla^2 c$ corresponding to a double-well free energy, although the solution can no longer be written in a simple form. We find that, for small e,

$$c_\infty(e) \approx c_{eq} + \frac{\chi \beta_0 Q c_{eq}}{2} \mathbf{E} \cdot \hat{\mathbf{n}} \tag{2.6}$$

where $c_{eq} = c_\infty(0)$ is the bulk concentration in zero field, $\chi = (\partial \mu / \partial c)_{eq}^{-1}$ is the zero-field susceptibility, and $Q = -(\partial \sigma / \partial c)_{eq}$. The quantity

$$\beta_0 Q c_{eq} \equiv \int_{-\infty}^{\infty} du [\sigma(c_0(u)) - \sigma(c_{eq})] \tag{2.7}$$

where $c_0(u)$ is the zero-field planar profile, is a direct measure of the order-parameter dependence of the mobility, with β_0 being a microscopic length of order ξ_0. For the "standard model" we have $c_{eq} = 1$, $\chi = 1/2$, $Q = 2$, and $\beta_0 = \sqrt{2}\, \xi_0$. The steady-state solution will be physically relevant only if it is stable against fluctuations in the bulk. This sets a lower (negative) bound on $\mathbf{E} \cdot \hat{\mathbf{n}}$, i.e., c_∞ must be larger than the spinodal value $c_{spinodal}$ ($= 1/\sqrt{3}$ for the "standard model"). In this paper we limit the discussion to small E so that $c_\infty > c_{spinodal}$.

3. MACROSCOPIC DESCRIPTION OF INTERFACIAL DYNAMICS

In this section we discuss the interfacial dynamics for small driving field at the macroscopic level. There are three ingredients: (i) the equation for the time evolution of the order parameter in the bulk, (ii) the analogue of the Gibbs–Thomson boundary condition, and (iii) an equation for the normal velocity of the interface. We show in the Appendix how to derive these ingredients in a systematic manner using the method of matched asymptotic expansions.[15–17] The essential feature of the derivation is an expansion in the ratio of the interfacial width to macroscopic length scales, to be defined below, which are determined by the curvature and the external field. In this section we quote results to first order in the expansion.

The first ingredient of the macroscopic description is the equation governing the order parameter in the bulk away from the interface, which becomes to leading order[22]

$$\frac{\partial \delta c}{\partial t} = 0 = \chi^{-1} [\nabla^2 \delta c \pm \mathbf{K} \cdot \nabla \delta c] \tag{3.1}$$

where the upper (lower) sign holds in the "plus" ("minus") phase, $\delta c(\mathbf{r}, t) \equiv c(\mathbf{r}, t) \mp c_{eq}$, and $\mathbf{K} \equiv \chi Q \mathbf{E}$. Note that $\mathbf{K}^{-1}$ is a macroscopic length scale related to the external field.[22,23] The corresponding current is

$$\mathbf{j} = -\chi^{-1}[\nabla \delta c \pm \mathbf{K}\, \delta c] \tag{3.2}$$

The bulk dynamics is essentially an expansion of Eq. (2.1) around the zero-field equilibrium values. Note that to first order the quasistatic approximation, $\partial \delta c / \partial t = 0$, holds in the bulk.

The second ingredient is the Gibbs–Thomson boundary condition. This relation gives the value of the order parameter near a curved or otherwise perturbed interface and is used as the interfacial boundary condition for the order parameter in a macroscopic description of the interfacial motion.[14,8] In the absence of a field, the Gibbs–Thomson boundary condition arises from a statement of local equilibrium, and the order parameter near the interface is determined by local quantities such as the local curvature and the local surface tension.

In the present situation the concept of local equilibrium is replaced by "local steady state." As shown in the Appendix, we may assume that, near the interface, structures with size on the order of the interfacial width will relax to their quasi stationary form on much smallar time scales than the time scales on which the position of the interface changes. In Section 2 we saw that the steady state of a planar interface depends on its orientation. The simplest assumption is that, for small distortions and external field, the effects of curvature and "tilt" are additive. As shown in the Appendix, this is indeed true to first order in the expansion.

We find that the Gibbs–Thomson boundary condition for the limiting order parameter as the interface is approached from the "plus" and "minus" phases is

$$\delta c_{\pm} = \chi \mu_{\pm} = \frac{c_{eq}}{2} d_0 \mathscr{K} \pm \frac{c_{eq}}{2} \beta_0 \mathbf{K} \cdot \hat{\mathbf{u}} \tag{3.3}$$

where $\hat{\mathbf{u}}$ is the local normal to the interface defined as pointing into the "plus" phase, and u is the signed distance from the interface. The curvature $\mathscr{K} = -\nabla \cdot \hat{\mathbf{u}}$ is defined as positive for a bump of the "plus" phase protruding into the "minus" phase. The microscopic capilliary length is $d_0 = \chi \Gamma / c_{eq}^2$ and the zero-field surface tension is $\Gamma = \xi_0^2 \int du [\partial_u c_0(u)]^2$, and β_0 is the microscopic length scale related to the c dependence of σ as defined in Section 2. Both d_0 and β_0 are order ξ_0. (In the "standard model" $d_0 = \xi_0 \sqrt{2}/3$ and $\beta_0 = \xi_0 \sqrt{2} = 3 d_0$.)

The first term on the RHS of Eq. (3.3) is independent of the side from which the interface is approached and is simply the equilibrium

Gibbs–Thomson boundary condition indicating that the order parameter near the macroscopically sharp interface is shifted by an amount proportional to the curvature. The external field **E** produces an additional term which depends on whether the interface is approached from the "plus" or "minus" phase. As will be shown, the new term in the boundary condition leads to an additional stabilizing mechanism when the field is tangential to the unperturbed interface. This new mechanism dominates the stability in that case.

The last ingredient is the expression for the normal velocity of the interface. We find that

$$v = \frac{1}{2c_{\text{eq}}}[j_u]_I + \frac{1}{2\chi}\beta_0 \mathscr{K}(\mathbf{K}\cdot\hat{\mathbf{u}}) \tag{3.4}$$

where j_u is the normal current and $[\bullet]_I = (\bullet)_+ - (\bullet)_-$ is the discontinuity across the interface (see footnote 3). The normal velocity v is defined as positive if the "minus" phase advances into the "plus" phase. Projecting Eq. (3.2) in the normal direction, we can rewrite Eq. (3.4) as

$$v = -\frac{1}{2\chi c_{\text{eq}}}[\partial_u \delta c]_I + \frac{1}{2\chi}\alpha_0 \mathscr{K}(\mathbf{K}\cdot\hat{\mathbf{u}}) \tag{3.5}$$

where $\alpha_0 \equiv \beta_0 - d_0$ is taken to be positive, as it is in the "standard model" ($\alpha_0 = 2d_0 = \xi_0 2\sqrt{2}/3$ in the "standard model").

The first term on the RHS of Eq. (3.4) is the discontinuity of the normal current which will appear even without the field. The second term in Eq. (3.4) is not present if the mobility is independent of the order parameter ($Q = 0$). As shown in the Appendix, this additional term is due to the variation in the tangential current along the interface, $\partial_s j_s$, and arises from the increased mobility near the interface. In zero field, $\partial_s j_s$ is higher order in the expansion, and, in the long-wavelength limit, is negligible relative to the discontinuity in the normal current.[37] We will show that the new mechanism represented by the second term of Eq. (3.4) determines the stability of the interface.

The orientational dependence of the surface current contribution to the normal velocity, i.e., the second term in Eq. (3.4), is shown schematically in Fig. 1. If $\mathbf{E}\cdot\hat{\mathbf{u}}$ is positive, the enhanced surface transport tends to smooth out small perturbations and the interface is stabilized, as shown in Fig. 1a. On the other hand, if $\mathbf{E}\cdot\hat{\mathbf{u}}$ is negative, as in Fig. 1b, the enhanced surface transport will amplify small perturbations, and the interface is destabilized. This orientation dependence differs from that which would obtain in an appropriately driven system if the Mullins–Sekerka instability

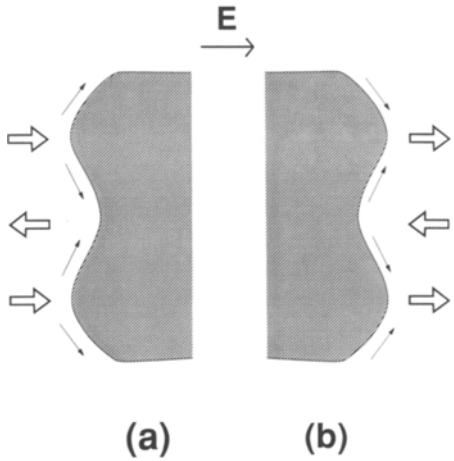

Fig. 1. Schematic diagram showing the effect of the surface current on a perturbed interface oriented normal to the field. The $c > 0$ region is shaded and the field drives positive c to the right. The small black arrows indicate the direction of current along the interface. The large white arrows indicate the motion of the interface. (a) A stable interface with respect to the surface currents. Due to the surface current, small bumps are rapidly filled in. (b) An unstable interface with respect to the surface currents. For this orientation, the surface current amplifies small bumps.

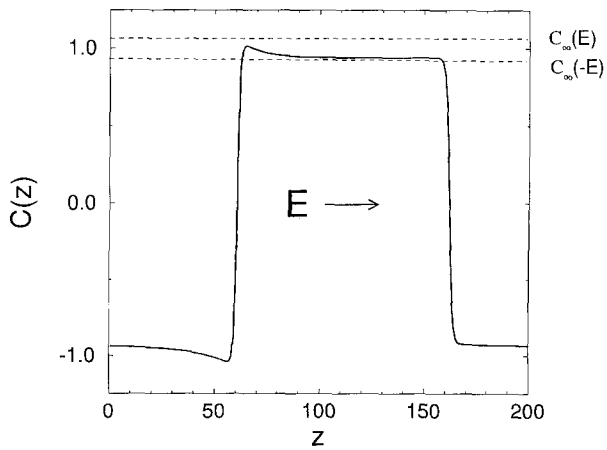

Fig. 2. The concentration profile of a kink–antikink pair. This profile is obtained from the numerical simulations described in Section 5. Such pairs occur if periodic boundary conditions are imposed in the field direction. The asymptotic order parameter values c_∞ are defined in Eq. (2.5). (Due partly to the curvature effects discussed in Section 3, the asymptotic values are not precisely reached.) Note that the bulk is undercooled on both sides of the left-hand interface. This interface would be unstable to displacements if a Mullins–Sekerka-like instability dominated.

dominates.[24] Consider, for example, Fig. 2, showing, in periodic boundary conditions, a kink–antikink pair. Notice that the left-hand interface separates undercooled bulks. One might expect the left-hand interface to exhibit a Mullins–Sekerka instability while the right-hand interface is expected to be stable. However, the new surface current mechanism has a stabilizing effect on the left-hand interface and succeeds in destabilizing the right-hand one.

2. LINEAR STABILITY ANALYSIS

With the macroscopic description provided in the previous section, we can consider the linear response of a flat interface to small perturbations. We assume now that we have an interface which, unperturbed, has its normal in the $\hat{\mathbf{n}}$ direction. We assume that far away from the interface, the order parameter is given by $\pm c_\infty$, where c_∞ is the steady-state bulk value given by Eq. (2.5) and depends on $\mathbf{E}\cdot\hat{\mathbf{n}}$. The interfacial dynamics is then given by Eqs. (3.1), (3.3), and (3.5).

Let the position of the unperturbed interface be $z=0$, with the "plus" phase occupying $z>0$. The position of the perturbed interface is given by $z(x,t)=h\exp(\omega_k t-ikx)$, where h is much smaller than k^{-1} and $|\mathbf{K}|^{-1}$. A perturbation of wavenumber k will grow (decay) if ω_k has positive (negative) real part. To first order in h, the curvature $\mathscr{K}$ is $-k^2h$ and the x component of the local normal is $u_x=ikh$. Let $\delta c_\pm = c\mp c_{\rm eq}$. We take a solution of the form

$$\delta c_\pm = \delta C_\pm \exp(\omega_k t - ikx \mp q_\pm z) \pm (c_\infty - c_{\rm eq})$$

in "plus" and "minus" phases, respectively. The additional term $c_\infty - c_{\rm eq}$ is due to the boundary condition far from the interface. The bulk dynamics [Eq. (3.1)] yields

$$0 = -(k^2 - q_\pm^2) - (K_z q_\pm \pm iK_x k) \tag{4.1}$$

where K_z and K_x are the z and x components of $\mathbf{K}=\chi Q\mathbf{E}$. To first order in h, the interfacial boundary condition (3.3) becomes

$$\delta C_\pm = -\frac{c_{\rm eq}}{2} d_0 k^2 h \pm \frac{ic_{\rm eq}}{2}\beta_0 K_x k h \tag{4.2}$$

while the expression for the normal velocity, Eq. (3.5), yields

$$2\chi c_{\rm eq}\omega_k h = q_+\delta C_+ + q_-\delta C_- - c_{\rm eq}\alpha_0 K_z k^2 h \tag{4.3}$$

Note that if the field **E** is tangent to the interface ($K_z = 0$), the surface current contribution to the normal velocity is negligible in the linear analysis and field effects are only in the modifications of the Gibbs–Thomson boundary condition and the bulk equation. On the other hand, if **E** is normal to the interface ($K_x = 0$), the modification of the boundary condition is negligible in the linear analysis, and the field effects are due to the surface current and the modification of the bulk equation.

Solving Eqs. (4.1)–(4.3) for ω_k gives

$$\omega_k = -\frac{k^2}{2\chi}\left(\alpha_0 K_z + \frac{K_x^2 \beta_0}{2q_1 - K_z} + d_0 q_1\right) \tag{4.4}$$

where $q_1 = (q_+ + q_-)/2$. Solving Eq. (4.1) and taking the roots with the positive real part, we find

$$q_\pm = \frac{K_z}{2} + \left(\frac{K_z^2}{4} + k^2 \pm iK_x k\right)^{1/2} \tag{4.5}$$

We consider specific cases. For $\mathbf{E} = 0$, we recover the usual zero-field result, $q_1 = k$ and $\omega_k = -d_0 k^3/(2\chi)$.[11,13] Since our choice of boundary conditions far from the interface corresponds to zero undercooling in the bulk, the interface is stable to perturbations of all wavenumbers. If the field is normal to the interface ($K_x = 0$), Eq. (4.4) becomes

$$\omega_k = -\frac{k^2}{2\chi}(\alpha_0 K_z + d_0 q_1) \tag{4.6}$$

Note that there is a contribution to the dispersion relation independent of q_1. Since q_1^{-1} is the length scale on which δc decays into the bulk, the physical origin of this term is independent of bulk gradients. This is the contribution from the surface current, and we see that, consistent with the analysis of Section 3, it stabilizes the interface if $K_z > 0$ and destabilizes the interface if $K_z < 0$. We first consider $K_z > 0$. The interface is linearly stable at all wavenumbers. In the limit of small k, $q_1 \simeq -K_z$ and $\omega_k \simeq -K_z \beta_0 k^2/(2\chi)$, where we have used $\alpha_0 + d_0 = \beta_0$. Note that the change in the asymptotic behavior, $\omega_k \sim -k^2$ rather then $\omega_k \sim -k^3$, indicates that the presence of the field strongly stabilizes the interface at long wavelengths (relative to the zero-field case).

For $K_z < 0$, whether the interface is linearly stable or unstable depends on the wavenumber of the perturbation. In the limit of small k, $q_1 \simeq -k^2/K_z$, so $\omega_k \simeq \alpha_0 K_z k^2/(2\chi)$ is positive, and the interface is unstable. At large k, $q_1 = k$, and we approach the zero-field result, $\omega_k = -d_0 k^3/(2\chi)$, making the interface stable. The wavenumber at which the interface is

marginally stable ($\omega_k = 0$) is $k = |K_z|(\alpha_0\beta_0)^{1/2} d_0^{-1}$. Typically in the linear regime and into the nonlinear regime, one observes patterns with characteristic size given by the wavelength at which the interface is maximally unstable, i.e., where ω_k is maximized.[1,5] The wavenumber at which this occurs is

$$k_{\max}^2 = K_z^2[2\beta_0\alpha_0 - d_0^2 + (\beta_0 + \alpha_0)(\beta_0\alpha_0 + d_0^2)^{1/2}]/(3d_0)^2$$

If the field is tangent to the interface ($K_z = 0$), the linear dispersion relation becomes

$$\omega_k = -\frac{k^2}{2\chi}\left(\frac{\beta_0 K_x^2}{2q_1} + d_0 q_1\right) \tag{4.7}$$

Independent of the sign of K_x, a field parallel to the interface will tend to stabilize the interface at all wavenumbers. That both terms in ω_k depend on q_1 indicates that the stabilization is due to a combination of the field effects in the bulk equation and the Gibbs–Thomson boundary condition. The behavior of the linear dispersion relation at small k is also different from the other cases. If $K_z > 0$, the field provides a length scale normal to the interface for the decay of δc to its bulk value and $q_1 \sim |K_z|$. For $\mathbf{K} = 0$, the only length scale is the tangential length-scale $|k|$ and we find $q_1 \sim |k|$. However, for $K_z = 0$ but $K_x \neq 0$, the field provides a length scale tangential to the interface only. We find that, in the limit of small k, $q_1 = (|K_x|\, k/2)^{1/2}$ and $\omega_k = -\beta_0 |K_x|^{3/2} k^{3/2}/(2\chi\sqrt{2})$. (An analysis without the orientational dependence of the boundary condition but with the modification of the bulk equation yields $\omega_k \sim -k^{5/2}$.[22]) Note that the behavior of ω_k at small k indicates that a tangential field will strongly stabilize the interface relative to the case of a normal field, and therefore, at long wavelengths, the interface tangential to the external field will be the most stable configuration. The results of the above discussion are illustrated in Fig. 3, in which the dispersion relations are shown for various values and orientations of the external field.

Our analysis can aid in understanding the results of previous numerical simulations. It has been observed that, in simulations of the phase ordering process in a continuum model of a driven diffusive system, the domains are roughly triangular, with the base of the triangle being the interface stable to the surface current mechanism ($\mathbf{E} \cdot \hat{\mathbf{u}} > 0$) while the sharp vertex is the unstable interface ($\mathbf{E} \cdot \hat{\mathbf{u}} < 0$).[31] Similar shapes have also been observed in simulations of fingering in driven diffusive systems.[33] These latter simulations have been carried out for a lattice system in the limit of large driving field, so comparisons with weak-field continuum models (such as the one discussed in the present work) have to be made cautiously.

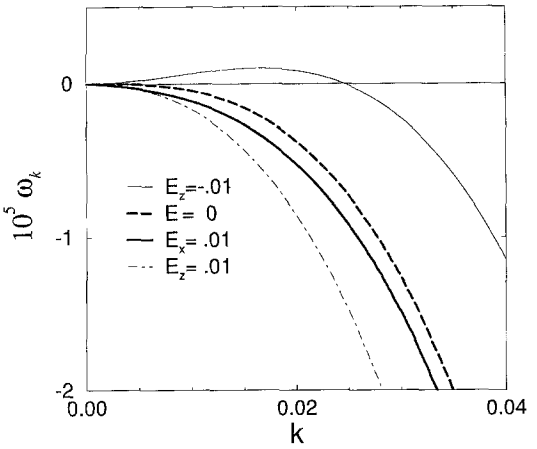

Fig. 3. The linear dispersion relation for several values and orientations of **E** for an interface with its normal in the $+z$ direction. Four values of **E** are shown ($\mathbf{E} = -0.01\hat{\mathbf{z}}$, $\mathbf{E} = 0$, $\mathbf{E} = 0.01\hat{\mathbf{z}}$, and $\mathbf{E} = 0.01\hat{\mathbf{x}}$). The parameters from the "standard model" are used. The interface is stable to perturbations of wavenumber k if $\omega_k < 0$ and unstable if $\omega_k > 0$. For small k, $\omega_k \sim -k^3$ if $\mathbf{E} = 0$. If the field is normal to the interface, $\omega_k \sim k^2$ if $E_z < 0$ and $\omega_k \sim -k^2$ if $E_z < 0$. If the field is tangential to the interface, $\omega_k \sim -k^{3/2}$.

Lattice effects will generally not be reproduced in a continuum description. However, it is worth noting that the shape of the strong-field fingers is consistent with the stability or instability as determined by the surface current (see Fig. 1).

The surface instability can also explain the reason (with the above caution) that under periodic boundary conditions, one always observes interfaces oriented tangentially to the field.[27-29] For periodic boundary conditions all interfaces must occur as kink–antikink pairs. If such a pair of interfaces has its normal in the field direction, the interface with $\mathbf{E} \cdot \hat{\mathbf{u}} < 0$ will be unstable to the surface instability discussed above. On the other hand, for the kink–antikink pair the interface with $\mathbf{E} \cdot \hat{\mathbf{u}} > 0$ will be undercooled. It will be unstable to the Mullins–Sekerka instability[24] at long wavelengths. For a very large system, this should dominate over the stabilizing effects of the surface current and hence the interface will also be unstable. Therefore our results indicate that a kink–antikink pair oriented normal to the field will always be unstable and cannot occur in the steady state, except for sufficiently small systems. (We note, however, that the maximal value of ω_k is much larger for the surface instability than for the Mullins–Sekerka instability for the kink–antikink pair, so that the unstable modes of the interface with $\mathbf{E} \cdot \hat{\mathbf{u}} < 0$ will grow significantly long before the Mullins–Sekerka instability affects the other interface.) In light of these

observations, additional Monte Carlo and continuum model simulations appear to be warranted.

For the steady-state interface oriented tangentially to the field, Monte Carlo simulations show the interfacial fluctuations are severely suppressed relative to the equilibrium interface, raising the possibility that, for the lattice model, the roughening temperature is raised to the nonequilibrium critical temperature.[34] Figure 4 shows schematically how the combination of the bulk drift current and the "tilt" term act to enhance the relaxation of the interface (when it is tangent to the field). Consider the negative order-parameter bump in Fig. 4. To the left of the bump, the value of c^2 is lowered due to the modification of the Gibbs–Thomson boundary condition. Due to the order-parameter dependent mobility, the drift (nondiffusive) current is larger for smaller c^2, making the bulk current larger on the left of the bump. On the right of the bump the opposite is true; c^2 is raised, and the bulk current is lowered. The net effect is to deposit positive order parameter into the negative-order parameter bump, thereby filling the bump and relaxing the interface. An analogous argument holds for the positive order-parameter bump, which is also filled, and therefore these effects act to relax the interface. Intuitively this enhanced relaxation suggests a suppression of interfacial roughness. However, to make a more definite statement requires the inclusion of noise and fluctuation effects, and connection with lattice models is subject to the usual cautions.

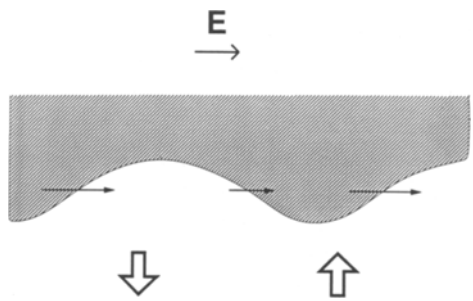

Fig. 4. A shematic showing the effect of the modification of the Gibbs–Thomson boundary condition for an interface oriented approximately parallel to the field. The symbols are the same as in Fig. 1, with the exception that the smaller arrows are the bulk order-parameter current rather than the surface current. Due to the orientational term in the boundary condition, the value of c^2 is smaller (larger) and therefore the current larger (smaller) where $\mathbf{E} \cdot \hat{\mathbf{u}}$ is negative (positive). The effect is to deposit c into the bump of the minus phase and pull positive c from a bump of the plus phase, thereby stabilizing the interface.

5. NUMERICAL RESULTS

We perform numerical simulations of the coarse-grained model to study the stability of the interface when it is approximately normal to the field. Equation (2.1) is integrated with the "standard model" chemical potential $\mu = -c + c^3 - \nabla^2 c$ and mobility $\sigma = 1 - c^2$. Periodic and antiperiodic boundary conditions in the field direction are considered. We find the orientation dependence of the stability agrees with our analysis of the surface-driven instability.

A discrete version of Eq. (2.1) on an $N \times N$ square lattice with $N = 100$ is treated here. A standard forward integration using an Euler scheme with a mesh size $\Delta x = 1$ and time interval $\Delta t = 0.01$ is used. We start with an approximately planar interface as our initial condition. To demonstrate the important stability features discussed in this paper, we need only study short times. In the figures for this section, we display integrations to time $t = 500$.

To model a nonzero flux at the boundaries one must consider an open system with, for example, periodic or antiperiodic boundary conditions in the direction of the field. We first consider antiperiodic boundary conditions in the field direction, which is consistent with a single interface or kink. Periodic boundary conditions are always employed in the direction transverse to the field. For $\mathbf{E} = 0$, the interface given by Eq. (2.4) is absolutely stable. However, if the flat interface is slightly perturbed in a nonzero field, we observe, depending on the orientation of $\mathbf{E}$, a stable interface if $\mathbf{E} \cdot \hat{\mathbf{u}} > 0$ (Fig. 5a) and an unstable interface if $\mathbf{E} \cdot \hat{\mathbf{u}} < 0$ (Fig. 5b). (In each case $|\mathbf{E}| = 0.1$.) The thick arrows in Fig. 5 indicate the motion of the interface in the two cases. Figure 5 also indicates with small arrows the incremental flux at each point in the lattice after subtracting off a gobally constant value equal to the flux at the boundaries. We observe that there is an accumulation of flux localized in the vicinity of the interface and directed along the interface. This incremental flux induced by $\mathbf{E}$ has been discussed in Sections 3 and 4 and is responsible for the stability properties of the interface. The interfacial profile along the central vertical line in Fig. 5 retains the qualitative features of Eq. (2.4). However, a complete numerical analysis of the interfacial boundary conditions discussed in Section 3 requires more extensive solutions.

In Fig. 6, we present the results of our simulation for the evolution of a kink–antikink pair with periodic boundary conditions. The external field is again normal to the unperturbed interfaces. The order parameter variation along the central line has been shown in Fig. 2. As discussed previously, the interface with $\mathbf{E} \cdot \hat{\mathbf{u}} > 0$ is undercooled. Hence, as argued in Section 3, the Mullins–Sekerka instability could act to destabilize the inter-

face having $\mathbf{E} \cdot \hat{\mathbf{u}} > 0$. The simulation shown in Fig. 6 is for a small system which effectively clamps the Mullins–Sekerka instability. Hence, in agreement with the antiperiodic case, the interfaces with $\mathbf{E} \cdot \hat{\mathbf{u}} > 0$ and $\mathbf{E} \cdot \hat{\mathbf{u}} < 0$ are stable and unstable, respectively, as indicated by the thicker arrows in Fig. 6.

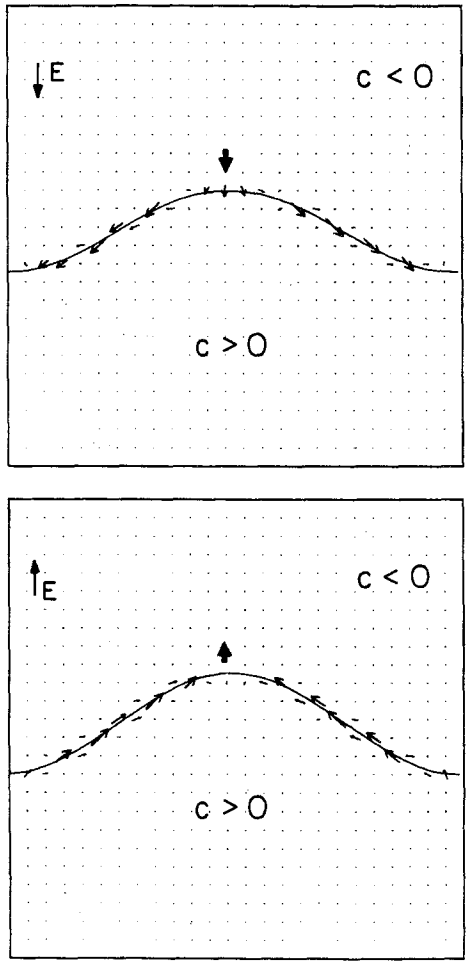

Fig. 5. Configurations obtained from a numerical simulation of Eq. (2.1) using antiperiodic boundary conditions. The normal $\hat{\mathbf{u}}$ is defined as pointing into the "plus" phase. The small arrows indicate the direction of incremental order-parameter current. The thicker arrows indicate the motion of the interface. There is an enhanced current (relative to the bulk) at the interface. In agreement with our analysis, the effect of the enhanced surface current is to stabilize the interface with $\mathbf{E} \cdot \hat{\mathbf{u}} > 0$ (upper figure) and destabilizes the interface with $\mathbf{E} \cdot \hat{\mathbf{u}} < 0$ (lower figure).

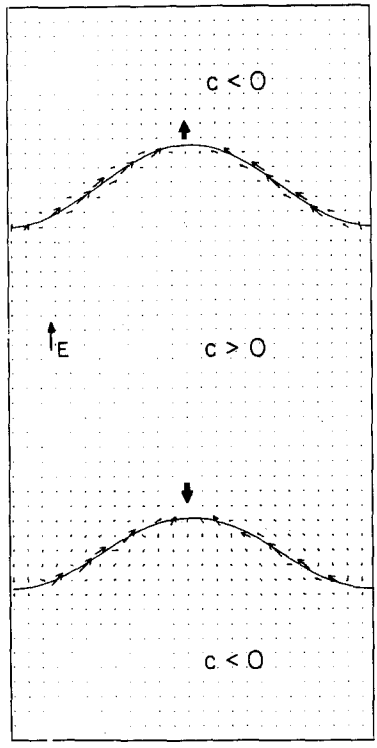

Fig. 6. A kink–antikink configuration obtained from a simulation of Eq. (2.1) using periodic boundary conditions. The symbols are the same as in Fig. 5. As shown by the thicker arrow, the orientational dependence of the interface stability is the same as that of Fig. 5, i.e., the interface is unstable if $\mathbf{E}\cdot\hat{\mathbf{u}}<0$ (the upper interface) and stable if $\mathbf{E}\cdot\hat{\mathbf{u}}>0$ (the lower interface).

From these examples, we conclude that the stability properties of the interfaces are determined primarily by their orientation with respect to the external field. Furthermore, the simulations reveal, in agreement with the analytic results of Section 3, that a new instability can be driven by an accumulation of flux in the vicinity of the interface.

6. SUMMARY

We studied the dynamics of an interface between two coexisting solid phases driven out of equilibrium by an applied field, which through the chosen boundary conditions induces a flux. Starting from the coarse-grained level of the Cahn–Hilliard equation, we showed that the external field has two important effects. First, it leads to an instability mechanism

localized to the vicinity of the interface. That is, in contrast with the more studied Mullins–Sekerka type instability, which involves differences in fluxes normal to the interface, the destabilization is due to flux along the interface itself. Second, the Gibbs–Thomson relation, which generally expresses a shift of the order parameter near an interface from its steady-state value, is modified, the external field producing a novel asymmetry in the shift. Each of these effects can determine the stability of the interface, depending on the orientation of the external field with respect to the interface.

Using the derived macroscopic description of the interfacial dynamics, we performed a linear stability analysis for a flat interface. We found that, if the external field is normal to the interface, the effect of the surface current is dominant. For the field pointing into the "plus" phase, the interface is stabilized, while for the field pointing into the "minus" phase, the field has a destabilizing effect. This orientational dependence is opposite what is expected if the Mullins–Sekerka mechanism dominated, i.e., leading to an unstable interface separating two undercooled bulks (see Fig. 2). If the external field is tangent to the interface, the modification of the Gibbs–Thomson relation is important and interfacial fluctuations are suppressed. This suggests an increase in the roughening temperature. More specifically, we determined the dispersion relation at small wavenumber k to be $\omega_k \sim \pm k^2$, with the sign depending on the direction of the field *normal* to the interface, and $\omega_k \sim -k^{3/2}$ if the field is *tangent* to the interface. These results are in agreement with Monte Carlo simulations of driven diffusive systems,[23,21,33,34] our numerical results expressed in Figs. 5 and 6, and with previous efforts on phase ordering.[31,32] We are presently performing a more thorough numerical study using the modified Cahn–Hilliard equation to test these results further.[38]

APPENDIX. DERIVATION OF INTERFACIAL EQUATIONS

In this Appendix we derive the interfacial equations from the coarse-grained description using the method of matched asymptotic expansions.[15–17] We use the method of Pego,[16] who derived the interfacial equations for zero field from the Cahn–Hilliard equation. We restate the bulk model of Section 2. The equation determining the order parameter $c(\mathbf{r}, t)$ is (2.1),

$$\frac{\partial c}{\partial t} = \nabla^2 \mu(c) - \mathbf{E} \cdot \nabla \sigma(c) \tag{A1}$$

where μ, the local (zero-field) chemical potential, is taken to be

$$\mu(c) = \mu_B(c) - \xi_0^2 \nabla^2 c \tag{A2}$$

in which μ_B does not contain any gradients and ξ_0 is a measure of the interfacial width. We assume Ising-like symmetry, so that μ_B is an odd function of c and $\pm c_{eq}$ are the equilibrium values of c. The order parameter current $\mathbf{j}$ is given by Eq. (2.3),

$$\mathbf{j} = -\nabla\mu(c) + \sigma(c)\,\mathbf{E} \tag{A3}$$

where $\sigma(c)$ is the order-parameter-dependent mobility, which is chosen to be a monotonically decreasing function of c^2. Without loss of generality we take $\sigma(c_{eq}) = 0$. (This corresponds to subtracting a constant current and does not affect the dynamics.) In this discussion we assume that, far from the interface, $c = \pm c_{eq} + \mathcal{O}(\xi_0)$, and hence $\mu = \mathcal{O}(\xi_0)$ far from the interface. (This precludes macroscopic undercooling in the present discussion.)

We treat ξ_0 as a small parameter and expand μ and c in powers of ξ_0,

$$\begin{aligned} \mu &= \mu_0 + \xi_0\mu_1 + \xi_0^2\mu_2 + \cdots \\ c &= c_0 + \xi_0 c_1 + \xi_0^2 c_2 + \cdots \end{aligned} \tag{A4}$$

Note that these expansions are not independent, since μ is a function of c. The mobility σ, order parameter current $\mathbf{j}$, and normal velocity of the interface v are functions of c and can be expanded in the same manner.

Time is rescaled as $\tau = \xi_0 t$ to extract the long-time behavior. The system is partitioned into bulk (outer) and interfacial (inner) regions. The interfacial region is defined as a skin around the interface of thickness larger than $\mathcal{O}(\xi_0)$ but less than the macroscopic lengths, which are $\mathcal{O}(1)$. Differential equations for c_i in terms of μ_i are obtained for each region and the solutions for c_i and μ_i are matched (to each order in ξ_0) at the boundary between the regions.

For the interfacial (inner) region, we use the time-dependent curvilinear coordinates defined as follows. Let $\hat{\mathbf{u}}$ and $\hat{\mathbf{s}}$ be the normal and tangent vectors at the interface point $\mathbf{r}(s)$ specified by the contour variable s. (For simplicity, we restrict the discussion to a one-dimensional interface in a two-dimensional bulk.) Then not too far from the interface a bulk point $\mathbf{r}$ can be represented by a pair (s, u), where $\mathbf{r} = \mathbf{r}(s) + u\hat{\mathbf{u}}(s)$. For the inner expansion we rescale the normal distance to the interface as $w = u/\xi_0$. Since $u \sim 1$ is the macroscopic length scale, we must match the inner solution to the outer solution at $1 \gg u \gg \xi_0$. In the limit of $\xi_0 \to 0$ this corresponds to matching the outer solution to the interface to the inner solution at w large. Following Pego,[16] we may write $c_i = \tilde{c}_i(u, \mathbf{r}, t)$ with

$\nabla_{\mathbf{r}}\tilde{c}_i$ in the $\hat{\mathbf{s}}$ direction. With this choice, $\partial_t c_i = \partial_t \tilde{c}_i + (\partial_t u)\,\partial_u \tilde{c}_i$, and the dynamical equation (A1) in the inner region becomes

$$\xi_0 \partial_\tau c - \frac{v}{\xi_0}\partial_w c = \frac{1}{\xi_0^2}\partial_w^2 \mu(c) - \frac{\mathscr{K}}{\xi_0}\partial_w \mu(c) - \frac{1}{\xi_0}(\mathbf{E}\cdot\hat{\mathbf{u}})\,\partial_w \sigma(c) + \partial_s^2 \mu(c) - (\mathbf{E}\cdot\hat{\mathbf{s}})\,\partial_s \sigma(c) \tag{A5}$$

where the curvature $\mathscr{K} = -\nabla\cdot\hat{\mathbf{u}}$ is positive for a bump of the "plus" phase into the "minus" phase. The normal velocity $v = -\partial_t u$ is positive if the "minus" phase advances into the "plus" phase. The velocity is also expanded in powers of ξ_0; $v = v_0 + \xi_0 v_1 + \mathcal{O}(\xi_0^2)$. In terms of c, the chemical potential is (dropping all tildes in the remainder of the discussion)

$$\begin{aligned}\mu(c) &= \mu_B(c) - \partial_w^2 c + \xi_0 \mathscr{K}\partial_w c - \xi_0^2 \partial_s^2 c \\ &= \mu_B(c_0) - \partial_w^2 c_0 + \xi_0[\mu_B' c_1 - \partial_w^2 c_1 + \mathscr{K}\partial_w c_0] + \cdots\end{aligned} \tag{A6}$$

where the prime indicates the derivative w.r.t. c evaluated at $c_0(w)$.

In the region far from the interface, we are interested in structures much larger than the interfacial width, so we use the unrescaled time-independent coordinate systems $\mathbf{r}$. In the outer region the dynamical equation (A1) is

$$\xi_0 \partial_\tau c = \nabla^2 \mu(c) - \mathbf{E}\cdot\nabla\sigma(c) \tag{A7}$$

where μ is given by Eq. (A2) and $\mathbf{j}$ by Eq. (A3). The outer solution μ_i^{outer} is matched to the same order in the inner solution μ_i^{inner}, but due to the rescaling of u in the inner region, the normal derivative of the outer solution $\partial_u \mu_i^{\text{outer}}$ is matched to the normal derivative at one order higher in the inner solution $\partial_w \mu_{i+1}^{\text{inner}}$. More generally, the matching condition is $\partial_u^m \mu_i^{\text{outer}} = \partial_w^m \mu_{i+m}^{\text{inner}}$ at the boundary between the outer and inner regions.

A1. Zeroth Order

In the inner (interfacial) region the dynamical equation to lowest order in ξ_0 (i.e., ξ_0^{-2}) is

$$0 = \partial_w^2 \mu_0 \tag{A8}$$

or $\mu_0 = a_0 + b_0 w$. The requirement that μ_0 and c_0 match an outer solution at $w \gg 1$ means that $\partial_w c_0$ vanishes at large w, μ_0 must be finite, and, hence, $b_0 = 0$. Making the analogy with a classical particle in a potential, the only solution with $\partial_w c_0 = 0$ at large w is the planar interfacial profile. Therefore

a_0 also vanishes, c_0 is the zero-field planar interface solution, and $\mu_0 = 0$ in the entire inner region.

In the outer (bulk) region the lowest order dynamical equation is

$$0 = \nabla^2 \mu_0 - \mathbf{E} \cdot \nabla c_0 \tag{A9}$$

The boundary condition far from the interface is $\mu_0 = 0$ and, from the inner solution, $\mu_0 = 0$ at the interface. The only solution meeting these boundary conditions is $\mu_0 = 0$, $c_0 = c_{eq}$ in the "plus" phase and $c_0 = -c_{eq}$ in the "minus" phase.

A2. First Order

The dynamical equation for the inner region [Eq. (A5)] to order ξ_0^{-1} is

$$-v_0 \partial_w c_0 = \partial_w^2 \mu_1 - \mathscr{K} \partial_w \mu_0 - (\mathbf{E} \cdot \hat{\mathbf{u}})\, \partial_w \sigma(c_0) \tag{A10}$$

where

$$\mu_1 = \mu_B' c_1 - \partial_w^2 c_1 + \mathscr{K} \partial_w c_0 \tag{A11}$$

Integrating Eq. (A10) w.r.t. w, we find

$$-v_0 c_0 = \partial_w \mu_1 - (\mathbf{E} \cdot \hat{\mathbf{u}})\, \sigma(c_0) + b_1 \tag{A12}$$

where we used the zeroth-order result $\mu_0 = 0$. We eliminate the even terms in Eq. (A12) by subtracting the expression evaluated for $w \to -\infty$ from its limiting value as $w \to \infty$,

$$-[v_0 c_0]_I = -2c_{eq} v_0 = [\partial_w \mu_1]_I \tag{A13}$$

where $[\bullet]_I$ indicates the discontinuity across the interface. However, v_0 must vanish since $\partial_w \mu_1$ at large w must be matched to the zeroth-order outer solution, $\partial_u \mu_0 = 0$. (This is consistent with no macroscopic undercooling.) Returning to Eq. (A12) and using $v_0 = 0$, $\sigma(c_{eq}) = 0$, and $\partial_w \mu_1 = 0$ at large w, we find that $b_1 = 0$.

Integrating Eq. (A12) w.r.t. w and using the above results, we find

$$\begin{aligned} \mu_1 &= a_1 + (\mathbf{E} \cdot \hat{\mathbf{u}}) \int_0^w dw'\, \sigma(c_0) \\ &= \mu_B' c_1 - \partial_w^2 c_1 + \mathscr{K} \partial_w c_0 \end{aligned} \tag{A14}$$

To obtain a_1 we multiply both sides of Eq. (A14) by $\partial_w c_0$ and integrate over the interface

$$a_1 \int dw\, \partial_w c_0 + (\mathbf{E}\cdot\hat{\mathbf{u}}) \int dw\, \partial_w c_0 \int_0^w dw'\, \sigma(c_0(w'))$$

$$= \int dw\, \partial_w c_0 (\mu_B' - \partial_w^2)\, c_1 + \mathscr{K} \int dw (\partial_w c_0)^2 \tag{A15}$$

The function $\partial_w c_0$ is the Goldstone mode corresponding to a translation of the interface. The first term on the RHS vanishes after integration by parts since the Goldstone mode is a zero eigenvector of the linear operator $\mu_B' - \partial_w^2$ (8, 39). The last term on the LHS of Eq. (A15) also vanishes since the integrand is odd. Solving for a_1 gives

$$a_1 = \frac{\Gamma}{2c_{\text{eq}}\xi_0}\mathscr{K} = \frac{c_{\text{eq}}}{2\chi}\frac{d_0}{\xi_0}\mathscr{K} \tag{A16}$$

where $\chi = (\partial u/\partial c)_{\text{eq}}^{-1}$ is the zero-field susceptibility, $d_0 = \chi\Gamma/c_{\text{eq}}^2$ is the microscopic capilliary length, and $\Gamma = \xi_0^2 \int dw (\partial_w c_0)^2$ is the zero-field surface tension. Note that d_0 is of order ξ_0.

The dynamical equation in the outer expansion is

$$0 = \nabla^2 \mu_1 - \mathbf{E}\cdot\nabla\sigma' c_1 \tag{A17}$$

In the outer region $c = \mu\chi$, where $\sigma' = \mp Q$, with $Q = -(\partial\sigma/\partial c)_{\text{eq}}$, so that

$$0 = \chi^{-1}\nabla^2 c_1 \pm Q\mathbf{E}\cdot\nabla c_1 \tag{A18}$$

This is the equation describing the bulk dynamics of the order parameter field to first order in ξ_0. Equation (A18) implies that, at this order in ξ_0, the quasistatic approximation $\partial_t c = 0$ in the bulk is valid.

Equation (A18) must be solved with the Gibbs–Thomson boundary condition at the interface. This is obtained by evaluating the inner solution for μ_1, Eq. (A14), at $w \to \pm\infty$,

$$c_1 = \chi\mu_1 = \frac{c_{\text{eq}}}{2}\frac{d_0}{\xi_0}\mathscr{K} \pm \frac{c_{\text{eq}}}{2}\frac{\beta_0}{\xi_0}\mathbf{K}\cdot\hat{\mathbf{u}} \tag{A19}$$

where $\mathbf{K}^{-1} \equiv (\chi Q\mathbf{E})^{-1}$ is a macroscopic length scale related to the external field and β_0 is a microscopic length scale of order ξ_0 defined by

$$\beta_0 Q c_{\text{eq}} \equiv \int_{-\infty}^{\infty} du\, \sigma(c_0(u))$$

[If $\sigma(c_{eq}) \neq 0$, then more generally, $\beta_0 Q\chi \equiv \int_{-\infty}^{\infty} du\,(\sigma(c_0(u)) - \sigma(c_{eq}))$.] The first term on the RHS of Eq. (A19) is even in u and is simply the equilibrium Gibbs–Thomson boundary condition indicating that the order parameter near the macroscopically sharp interface is shifted by an amount proportional to the curvature. The external field **E** produces an additional term which is asymmetric in u and therefore depends on whether the interface is approached from the "plus" or "minus" phase. As shown in Section 4, this new term in the boundary condition leads to an additional stabilizing mechanism when the field is tangential to the interface. This new mechanism dominates the stability in that case.

A3. Second Order

To complete the first-order description in the bulk, we must obtain $\partial_w \mu_2$ in the inner solution evaluated at large w. The dynamical equation for the inner expansion [Eq. (A5)] to order ξ_0^0 is

$$-v_1 \partial_w c_0 = \partial_w^2 \mu_2 - \mathscr{K} \partial_w \mu_1 + \partial_s^2 \mu_0 - (\mathbf{E} \cdot \hat{\mathbf{u}})\, \partial_w \sigma' c_1 - (\mathbf{E} \cdot \hat{\mathbf{s}})\, \partial_s^2 \sigma(c_0) \tag{A20}$$

The second-order chemical potential is related to c_i by

$$\mu_2 = \tfrac{1}{2}\mu_B'' c_1^2 + \mu_B' c_2 - \partial_w^2 c_2 + \mathscr{K} \partial_w c_1 - \partial_s^2 c_0 \tag{A21}$$

Integrating Eq. (A20) over the interface and using the lower-order results, we obtain

$$\begin{aligned} -2v_1 c_{eq} &= [\partial_w \mu_2 - (\mathbf{E} \cdot \mathbf{u})\, \sigma' c_1]_I - \mathscr{K} [\mu_1]_I \\ &= [\partial_w \mu_2 - (\mathbf{E} \cdot \mathbf{u})\, \sigma' c_1]_I - \mathscr{K} (\mathbf{E} \cdot \hat{\mathbf{u}}) \frac{\beta_0 Q c_{eq}}{\xi_0} \\ &= [\partial_w \mu_2 - (\mathbf{E} \cdot \mathbf{u})\, \sigma' c_1]_I - \mathscr{K} (\mathbf{K} \cdot \hat{\mathbf{u}}) \frac{\beta_0 c_{eq}}{\chi \xi_0} \end{aligned} \tag{A22}$$

where we use Eq (A19) for the discontinuity in μ_1 across the interface. We can recognize the physical significance of this by noticing that we can expand the current (in the inner solution) as $\mathbf{j} = \xi_0^{-1}\mathbf{j}_{-1} + \mathbf{j}_0 + \xi_0 \mathbf{j}_1 + \cdots$, where $\mathbf{j}_{-1} = -\hat{\mathbf{u}} \partial_w \mu_0 = 0$, $\mathbf{j}_0 = -\hat{\mathbf{u}} \partial_w \mu_1 + \mathbf{E}\sigma(c_0)$, and $\mathbf{j}_1 = -\hat{\mathbf{u}} \partial_w \mu_2 - \hat{\mathbf{s}} \partial_s \mu_1 + \mathbf{E}\sigma' c_1$. We identify $j_{1,u} = -\partial_w \mu_2 + (\mathbf{E} \cdot \hat{\mathbf{u}})\, \sigma' c_1$ and

$$\begin{aligned} \frac{1}{\xi_0} \int_{-\infty}^{\infty} dw\, \partial_s j_{0,s} &= -\frac{1}{\xi_0} \partial_s (\mathbf{E} \cdot \hat{\mathbf{s}}) \int_{-\infty}^{\infty} dw\, \sigma(c_0(w)) \\ &= (\mathbf{E} \cdot \hat{\mathbf{u}})\, \mathscr{K} \frac{\beta_0 Q c_{eq}}{\xi_0} = (\mathbf{K} \cdot \hat{\mathbf{u}}) \frac{c_{eq} \beta_0}{\chi \xi_0} \mathscr{K} \end{aligned} \tag{A23}$$

Since $v = \xi_0 v_1 + \mathcal{O}(\xi_0^2)$ and $[j_u]_I = \xi_0 [j_{1,u}] + \mathcal{O}(\xi_0^2)$, we can write the normal velocity as

$$v = \frac{1}{2c_{\text{eq}}} [j_u]_I + \frac{1}{2c_{\text{eq}}} \int_{-\infty}^{\infty} dw\, \partial_s j_s + \mathcal{O}(\xi_0^2)$$

$$= \frac{1}{2c_{\text{eq}}} [j_u]_I + \mathscr{K}(\mathbf{K} \cdot \hat{\mathbf{u}}) \frac{\beta_0}{2\chi} + \mathcal{O}(\xi_0^2) \tag{A24}$$

In other words, in addition to the usual discontinuity in the normal current, there is also a contribution to the normal velocity due to the tangential derivative of the tangential current.

A4. Kinetic Corrections to μ_2

We can also use the method of matched asymptotic expansions to obtain higher-order corrections to the macroscopic boundary condition. At the next order the Gibbs–Thomson boundary condition has a contribution proportional to the normal velocity. Integrating Eq. (A20) twice w.r.t. w, we obtain

$$\mu_2 = -v_1 \int_0^w dw'\, c_0(w') + \mathscr{K} \int_0^w dw'\, \mu_1 - (\mathbf{E} \cdot \hat{\mathbf{u}}) \int_0^w dw'\, \sigma' c_1 + b_2 w + a_2$$

$$= \tfrac{1}{2} \mu_B'' c_1^2 + \mu_B' c_2 - \partial_w^2 c_2 + \mathscr{K} \partial_w c_1 \tag{A25}$$

We need to obtain the value of a_2 which will enter the Gibbs–Thomson boundary condition. To do so, we eliminate the c_2 dependence by multiplying by the Goldstone mode $\partial_w c_0$ (i.e., the zero eigenvector of $\mu_B' - \partial_w^2$) and integrating across the interface. This procedure also eliminates all the odd terms in w in Eq. (A25). Using Eq. (A14) for μ_1, we find

$$2c_{\text{eq}} a_2 = 2v_1 \int_0^{\infty} dw (c_{\text{eq}} - c_0)\, c_0$$

$$+ (\mathbf{E} \cdot \hat{\mathbf{u}}) \int_{-\infty}^{\infty} dw\, \partial_w c_0 \int_0^w dw' [\sigma' c_1 + \mathscr{K} \sigma(c_0)]$$

$$- \int_{-\infty}^{\infty} dw\, \partial_w c_0 \left(\frac{1}{2} \mu_B'' c_1^2 + \mathscr{K} \partial_w c_1 \right) \tag{A26}$$

Equation (A25) contains linear divergences for large $|w|$. These terms match $\partial_u \mu_1^{\text{outer}}$ and must be subtracted off when obtaining the matching condition for μ_2 in the outer expansion. We evaluate the "subtracted" μ_2 at large w. This leads to a very complicated boundary condition for $c_2 = \mu_2 \chi$ at the outer expansion,

$$\chi^{-1}c_2 = \frac{v_1}{c_{eq}}\int_0^{\infty} dw(c_{eq}^2 - c_0^2) + \mathscr{K}\int_0^{\pm\infty} dw'(\mu_1 - \mu_{1,\pm})$$
$$-(\mathbf{E}\cdot\hat{\mathbf{u}})\int_0^{\pm\infty} dw'(\sigma' c_1 \pm Q c_{1,\pm})$$
$$+\frac{1}{2c_{eq}}\int_{-\infty}^{\infty} dw\, \partial_w c_0 \left[\frac{1}{2}\mu_B'' c_1^2 - \mathscr{K}\partial_w c_1 + (\mathbf{E}\cdot\hat{\mathbf{u}})\int_0^{w} dw'\, \sigma' c_1\right] \tag{A27}$$

where the subscript $\pm$ indicates that the expression is evaluated as one approaches the interface from the "plus" or "minus" phase and $Q = -(\partial\sigma/\partial c)_{eq}$. Therefore at $\mathcal{O}(\xi_0^2)$ there is a kinetic contibution (the term proportional to v_1) to the Gibbs–Thomson boundary condition. For $\mathbf{E} = 0$, c_1 is an even function of u, μ_1 is independent of u, and the boundary condition simplifies to

$$\chi^{-1}c_2 = \frac{v_1}{c_{eq}}\int_0^{\infty} dw(c_{eq}^2 - c_0^2) \tag{A28}$$

Hence, for $\mathbf{E} = 0$, only the kinetic contribution survives at this order.

The kinetic contribution may be important in the case where the bulk is supercooled by an amount larger than $\mathcal{O}(\xi_0)$. For $\mathbf{E} = 0$ the dynamical equations to first order in ξ_0 [Eqs. (A18), (A19), and (A24)] are analogous to the equations describing Hele–Shaw flow.[1,2] Such an analogy has also been noted between crystal growth and Hele–Shaw flow.[40]. We find, however, that if the supercooling in the bulk is larger than $\mathcal{O}(\xi_0)$, i.e., if there is a macroscopic supercooling, v_0 will be nonzero and there will be a kinetic contribution to the boundary condition for μ_1. Therefore, even at first order in ξ_0, the analogy with Hele–Shaw flow is not complete.

A5. First Order Macroscopic Equations: Summary

The equations describing the interfacial dynamics to first order in ξ_0 are as follows:

(i) The bulk dynamics is given by Eq. (A18),

$$0 = \chi^{-1}[\nabla^2\delta c \pm \mathbf{K}\cdot\nabla\delta c] \tag{A29}$$

where $\mathbf{K} = \chi Q\mathbf{E}$, $Q = -(\partial\sigma/\partial c)_{eq}$, $\chi^{-1} = (\partial\mu/\partial c)_{eq}$, and $\delta c = c \mp c_{eq}$.

(ii) This equation must be solved with the boundary condition at the interface given by Eq. (A19),

$$\delta c_{\pm} = \frac{c_{eq}}{2} d_0\mathscr{K} \pm \frac{c_{eq}}{2}\beta_0(\mathbf{K}\cdot\hat{\mathbf{u}}) \tag{A30}$$

where $d_0 \equiv \chi\Gamma/c_{eq}^2$, Γ is the zero-field surface tension, and $\beta_0 Q c_{eq} \equiv \int du\,[\sigma(c_0(u)) - \sigma(c_{eq})]$.

(iii) The interfacial velocity is given by Eq. (A24),

$$v = \frac{1}{2c_{eq}}[j_u]_I + \mathscr{K}(\mathbf{K}\cdot\hat{\mathbf{u}})\frac{\beta_0}{2\chi} \tag{A31}$$

The bulk current is $\mathbf{j} = -\chi^{-1}(\nabla\delta c \pm \mathbf{K}\delta c)$. Combining this with Eqs. (A24) and (A19), we find for the normal velocity of the interface

$$v = -\frac{1}{2\chi c_{eq}}[\partial_u \delta c]_I + \mathscr{K}(\mathbf{K}\cdot\hat{\mathbf{u}})\frac{\alpha_0}{2\chi} \tag{A32}$$

where $\alpha_0 \equiv \beta_0 - d_0$ is taken to be positive as in the "standard model." Equations (A29), (A30), and (A32) completely define the macroscopic dynamics to first order in ξ_0.

ACKNOWLEDGMENTS

We gratefully acknowledge Dr. Timothy Rogers for his important insights and valuable discussions in the early stages of this work. We also thank Prof. Yoshitsugu Oono for helpful discussions. J.L.M. and A.H.M. are grateful for the support of the Direccion General de Investigacion Cientifica y Tecnica (Spain), Pro. No. PBR87-0014. D.J. and C.Y. thank the National Science Foundation for support through the Division of Materials Research under Grant No. DMR89-14621. A.H.M., C.Y., and D.J. also thank NATO for partial support under the Collaborative Research Grant No. 900328. Finally, we wish to thank the referees for a very careful reading of the manuscript and valuable comments.

REFERENCES

1. J. S. Langer, in *Proceedings of Les Houches Summer School: Chance and Matter*, J. Soulette *et al.*, eds. (Elsevier, New York, 1987).
2. D. A. Kessler, J. Koplik, and H. Levine, *Adv. Phys.* **35**:255 (1988).
3. P. Pelcé, ed., *Dynamics of Curved Fronts* (Academic Press, London, 1988).
4. D. Bensimon, L. P. Kadanoff, S. Liang, B. I. Schraiman, and Ch. Tang, *Rev. Mod. Phys.* **58**:977 (1986).
5. J. V. Maher, *Phys. Rev. Lett.* **54**:1498 (1985); M. W. DeFrancesco and J. V. Maher, *Phys. Rev. A* **39**:4709 (1989).
6. G. Tryggvason and H. Aref, *J. Fluid Mech.* **136**:1 (1983); **154**:287 (1985).
7. J. Casademunt and D. Jasnow, *Phys. Rev. Lett.* **67**:3677 (1991); J. Casademunt, D. Jasnow, and A. Hernàndez-Machado, *Int. J. Mod. Phys. B* **6**:1647 (1992).

8. D. Jasnow, in *Phase Transitions and Critical Phenomena*, Vol. 10, C. Domb and J. L. Lebowitz, eds. (Academic Press, New York, 1986), p. 269, and references cited therein.
9. W. W. Mullins and R. F. Sekerka, *J. Appl. Phys.* **35**:444 (1964).
10. P. G. Saffman and G. I. Taylor, *Proc. R. Soc. A* **245**:312 (1958).
11. D. Jasnow and R. K. P. Zia, *Phys. Rev. A* **36**:2243 (1987); Y. Oono and A. Shinozaki, University of Illinois, preprint (1992).
12. B. Derrida, J. L. Lebowitz, E. R. Speer, and H. Spohn, *Phys. Rev. Lett.* **67**:165 (1991).
13. J. S. Langer and L. A. Turski, *Acta. Metall.* **25**:1113 (1977); D. Jasnow, D. A. Nicole, and T. Ohta, *Phys. Rev. A* **23**:3192 (1981).
14. K. Kawasaki and T. Ohta, *Prog. Theor. Phys.* **68**:129 (1982); K. Kawasaki and T. Ohta, *Physica A* **118**:175 (1983); T. Ohta, *Ann. Phys.* **158**:31 (1984).
15. G. Caginalp, *Ann. Phys.* (N.Y.) **172**:136 (1986); G. Caginalp and P. C. Fife, *SIAM J. Appl. Math.* **48**:506 (1988); G. Caginalp, *Phys. Rev. A* **39**:5887 (1989).
16. R. L. Pego, *Proc. R. Soc. Lond. A* **422**:261 (1989).
17. L. Bronsard and R. V. Kohn, *J. Differential Equations* **90**:211 (1991).
18. H. K. Janssen and B. Schmittmann, *Z. Phys. B* **63**:517 (1986).
19. H. K. Janssen and B. Schmittmann, *Z. Phys. B* **64**:503 (1986).
20. K.-t. Leung and J. L. Cardy, *J. Stat. Phys.* **44**:567 (1986).
21. K.-t. Leung, B. Schmittmann, and R. K. P. Zia, *Phys. Rev. Lett.* **62**:1772 (1989).
22. A. Hernàndez-Machado and D. Jasnow, *Phys. Rev. A* **37**:656 (1988).
23. K.-t. Leung, *J. Stat. Phys.* **50**:405 (1988).
24. K.-t. Leung, *J. Stat. Phys.* **61**:345 (1990).
25. R. K. P. Zia and K.-t. Leung, *J. Phys. A* **24**:1399 (1991).
26. A. Hernàndez-Machado, H. Guo, J. L. Mozos, and D. Jasnow, *Phys. Rev. A* **39**:4783 (1989).
27. S. Katz, J. L. Lebowitz, and H. Spohn, *Phys. Rev. B* **28**:1655 (1983); *J. Stat. Phys.* **34**:497 (1984).
28. J. Krug, J. L. Lebowitz, H. Spohn, and M. Q. Zang, *J. Stat. Phys.* **44**:535 (1986); R. Dickman, *Phys. Rev. A* **38**:2588 (1988); J. Krug, *Phys. Rev. Lett.* **67**:1882 (1991).
29. L. Vallés and J. Marro, *J. Stat. Phys.* **43**:441 (1986); **49**:89, 121 (1987); J. Marro, J. L. Vallés, and J. M. Gonzalez-Miranda, *Phys. Rev. B* **35**:3372 (1987).
30. K. Kitahara, Y. Oono, and D. Jasnow, *Mod. Phys. Lett. B* **2**:765 (1988).
31. C. Yeung, T. Rogers, A. Hernàndez-Machado, and D. Jasnow, *J. Stat. Phys.* **66**:1071 (1992).
32. S. Puri, K. Binder, and S. Dattagupta, *Phys. Rev. B* **46**:98 (1992).
33. D. H. Boal, B. Schmittman, and R. P. K. Zia, *Phys. Rev. A* **43**:5214 (1991).
34. K.-t. Leung, K. K. Mon, J. L. Vallés, and R. K. P. Zia, *Phys. Rev. Lett.* **61**:1744 (1988); *Phys. Rev. B* **39**:9312 (1989).
35. J. W. Cahn and H. E. Hilliard, *J. Chem. Phys.* **28**:258 (1958); H. E. Cook, *Acta Metall.* **18**:297 (1970).
36. J. D. Gunton, M. san Miguel, and P. S. Sahni, in *Phase Transitions and Critical Phenomena*, Vol. 8, C. Domb and J. L. Lebowitz, eds. (Academic Press, New York, 1983), p. 267; H. Furukawa, *Adv. Phys.* **34**:703 (1985); K. Binder, in *Phase Transformations of Materials* (*Materials Science and Technology*), Vol. 5, P. Haasen, ed., p. 405 (Springer-Verlag, Berlin, 1991).
37. T. Ohta, *J. Phys. C* **21**:L361 (1988).
38. J. L. Mozos and A. Hernàndez-Machado, in preparation (1992).
39. T. Rogers, Ph.D. Thesis, University of Toronto (1989).
40. P. Pelce and A. Pumir, *J. Cryst. Growth* **73**:337 (1985); P. Pelce, *Europhys. Lett.* **7**:453 (1988).